

LA-5427-MS

INFORMAL REPORT

C.3

CIC-14 REPORT COLLECTION
**REPRODUCTION
COPY**

PACER Program

A Strong Explosion in a Spherical Cavity:
Two-Dimensional Evolution



los alamos
scientific laboratory
of the University of California
LOS ALAMOS, NEW MEXICO 87544

UNITED STATES
ATOMIC ENERGY COMMISSION
CONTRACT W-7405-ENG. 36

This report was prepared as an account of work sponsored by the United States Government. Neither the United States nor the United States Atomic Energy Commission, nor any of their employees, nor any of their contractors, subcontractors, or their employees, makes any warranty, express or implied, or assumes any legal liability or responsibility for the accuracy, completeness or usefulness of any information, apparatus, product or process disclosed, or represents that its use would not infringe privately owned rights.

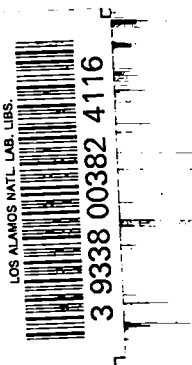
In the interest of prompt distribution, this LAMS report was not edited by the Technical Information staff.

LA-5427-MS
Informal Report
SPECIAL DISTRIBUTION
ISSUED: October 1973



Los Alamos
scientific laboratory
of the University of California
LOS ALAMOS, NEW MEXICO 87544

PACER Program
A Strong Explosion in a Spherical Cavity:
Two-Dimensional Evolution



by
Eric M. Jones



ABSTRACT

A 100 kiloton explosion in a spherical cavity of 200 m radius, air-filled, has been calculated. It is found that the hot, low density bubble rises at about 18 m/sec. At 12 seconds the bubble is near the top wall and has a temperature of at least 1900 K.

PACER PROGRAM

A STRONG EXPLOSION IN A SPHERICAL CAVITY:

TWO-DIMENSIONAL EVOLUTION

by

Eric M. Jones

I. INTRODUCTION

At the suggestion of Forrest Gilmore of R&D Associates and members of Group T-3 of the Los Alamos Scientific Laboratory, the two-dimensional atmospheric fireball program, YAQUI,^{1,2} has been modified to enable treatment of the evolution of a nuclear fireball in a spherical cavity.

It has been proposed that a large cavity be dug in a salt dome filled with a working fluid and used to store the energy of a nuclear explosion for subsequent extraction and conversion to electrical energy. Some of the physics questions arising from the initial feasibility studies are:

1) What are the circulation patterns generated by buoyant rise of the fireball, and

2) How hot is the fireball when it first comes into contact with the top of the cavity?

Preliminary answers to these questions are addressed by the first calculation. Limitations imposed by the numerics and by the physics assumptions preclude satisfactory treatment of the late evolution of the flow field.

II. INITIAL CONDITIONS

The cavity is assumed to be 196 m in radius. The ambient fluid is dry air at 0.2027 g/cm^3 density and specific internal energy $5.658 \times 10^9 \text{ erg/g}$ (767 K). The spherical radiation-hydrodynamics program, RADFLO,³ has been used by Zinn and Kodis⁴ to calculate the initial fireball produced by a 100 kt nuclear explosion. Figures 1 and 2 show profiles of density, ρ , and temperature, T , at 0.15 sec after the event. At this time three physically important conditions have been achieved:

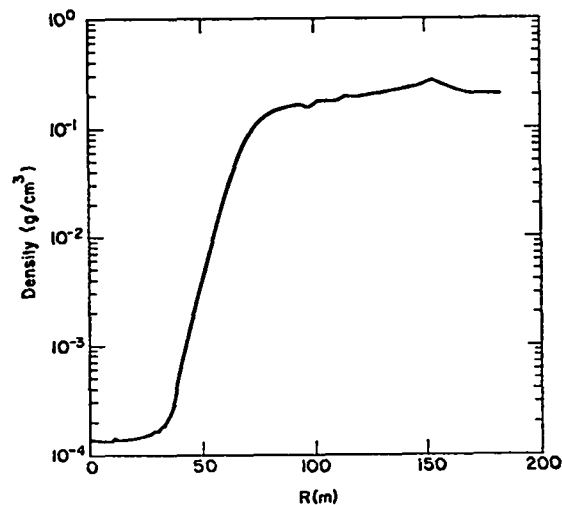


Fig. 1. Density profile in the spherical cavity at 0.15 sec after the explosion. The shock wave has almost reached the wall.

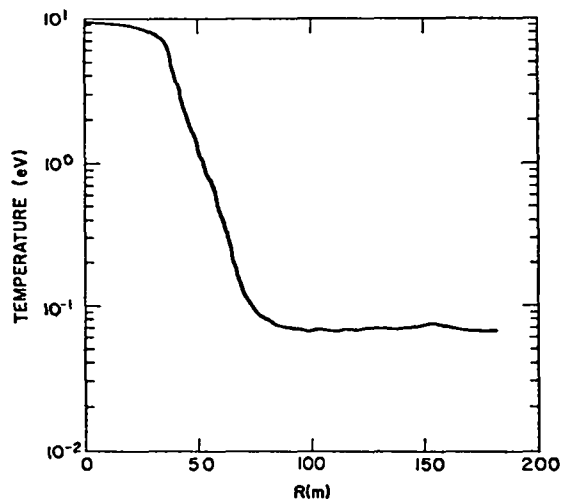


Fig. 2. Temperature profile computed by RADFLO at 0.15 sec after the explosion.

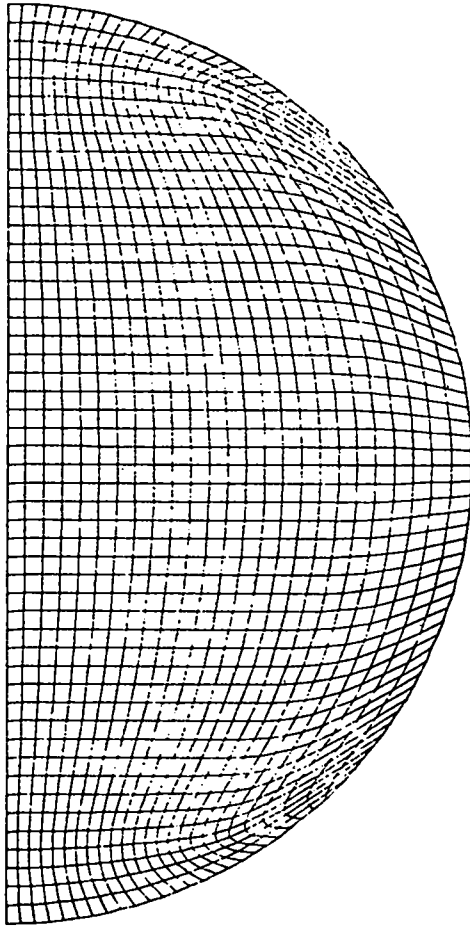


Fig. 3. The Eulerian computing grid.

1) The cavity is virtually in pressure equilibrium except for a 245 bar peak overpressure in the shock,

2) the shock front has almost reached the cavity wall, and

3) growth of the fireball is completely dominated by hydrodynamic motions rather than radiation transport. (RADFLO calculations show this to be true after a few microseconds.)⁵

The computing mesh was generated by a method developed by Hirt and Amsden.⁶ A grid of $25 \times 50 = 1250$ computing cells has been generated with exterior vertices equal spaces on a 196-m radius semicircle. The average cell is 8 m on a side. The grid is reproduced in Fig. 3.

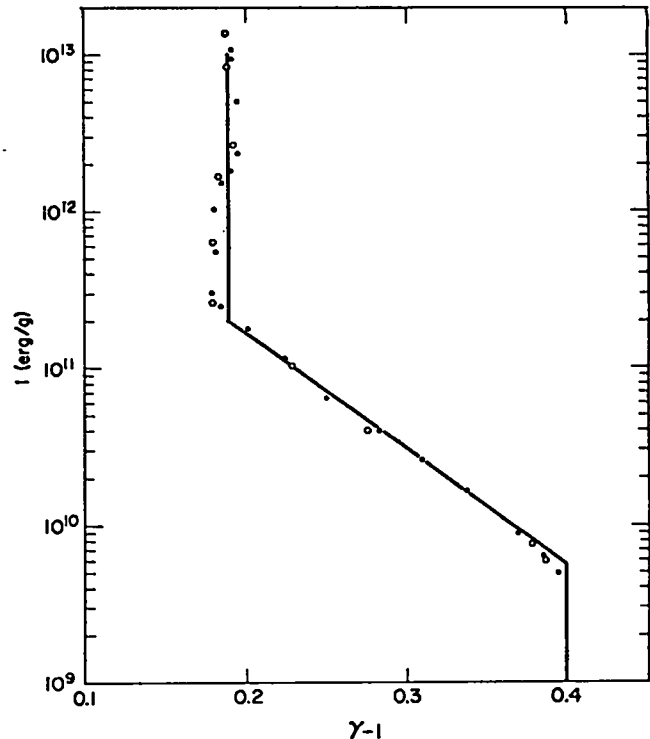


Fig. 4. The assumed equation of state. The points are taken from RADFLO output at two times. The solid curves are analytic fits used in the YAQUI calculation.

YAQUI uses cell-centered densities, ρ , pressures, P , and specific internal energy, I , while velocities are defined at cell vertices. RADFLO results have been linearly interpolated to the appropriate positions in the YAQUI grid.

The fact of pressure equilibrium has simplified definition of the equation of state. Pressure is a monotonic function of I or ρ . Figure 4 shows values of $\gamma-1 = P/\rho I$ extracted from the RADFLO output and the adopted analytic fit. The transition points are at $I = 6 \times 10^9$ and 2×10^{11} erg/g. Figure 5 presents a temperature-specific internal energy relation.

Briefly, the initial configuration consists of a hollow, spherical bubble of 70-m radius at 9-eV temperature and central density of $\rho = 1.4 \times 10^{-4}$ g/cm³ ($\rho/\rho_0 = 7 \times 10^{-4}$). A spherical shock wave has almost reached the outer boundary.

A no-slip, perfectly reflecting boundary has been assumed. In detail, state variables P , ρ , and

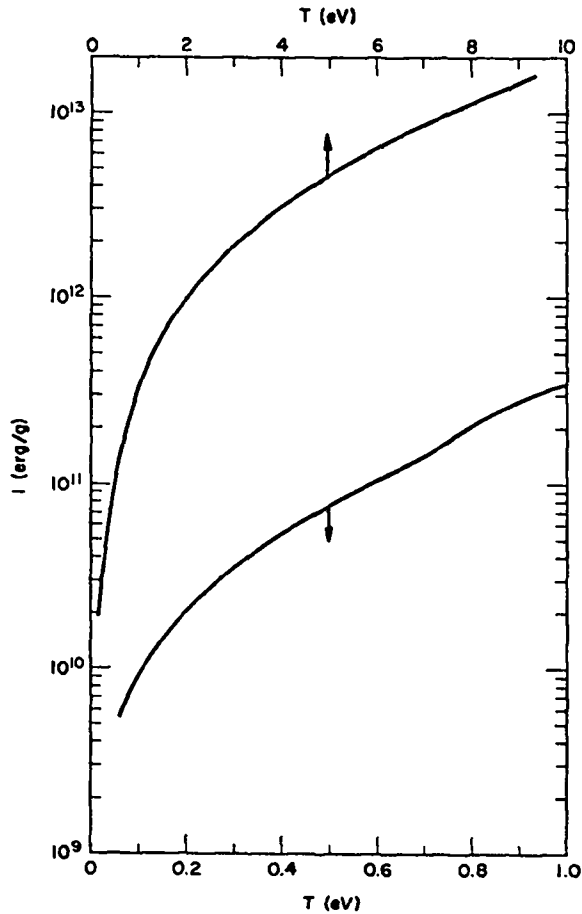


Fig. 5. Temperature (T) vs specific internal energy (I). Note that the lower curve refers to temperatures up to 1 eV while the upper curve extends to 10 eV.

I are matched across the boundary, and both velocity components are set to zero at the boundary.

III. THE FLOW FIELD

The evolving flow field is complex. Initially we have a virtually stationary fireball with a shock wave bouncing back and forth between the origin and the cavity wall. The shock wave period is about 0.46 sec. However, the hollow bubble is buoyant. To first order it should achieve an equilibrium rise rate

$$U = \frac{2}{3} \sqrt{Rg}.$$

Taking $g = 10 \text{ m/sec}$ and $R = 70 \text{ m}$, we have $U \approx 18 \text{ m/sec}$.

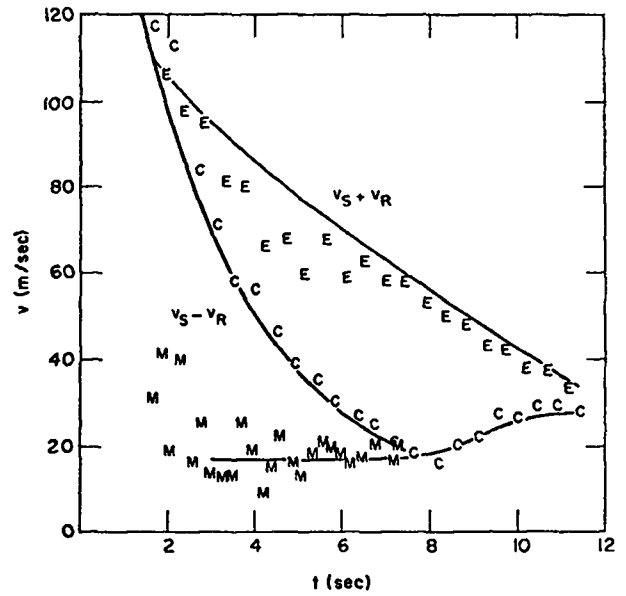


Fig. 6. Velocity extremes produced by interaction of the reverberating shock wave and the buoyantly rising fireball. See text.

A further complication arises when one considers that as the hot, hollow bubble rises the reflected shock wave no longer "sees" a spherically symmetric configuration. Consider the situation after the bubble has risen some distance from the cavity center. The part of the shock wave that reflects off the top of the cavity traverses ambient fluid for a while but soon encounters the off-center, hot bubble. Because the sound speed in the bubble is higher than the ambient sound speed, this part of the reflected shock wave speeds up for a while. The part of the shock wave reflected from the bottom of the cavity traverses only ambient fluid.

The flow pattern during the transition from purely radial motion to a smooth circulation pattern can be partially disentangled. We identify a characteristic rise speed, v_R , and a characteristic particle speed in the shock, v_S . We further identify the maximum speed in the mesh, v_{MAX} . As time advances v_{MAX} shows two types of maxima and one type of minimum. The minima occur when the shock front is stationary at the wall or the center. Early in the calculation $v_R \approx 0$ and v_{MAX} represents material motion behind the shock front, but later $v_{MAX} \approx v_R$. The maxima occur when the shock wave

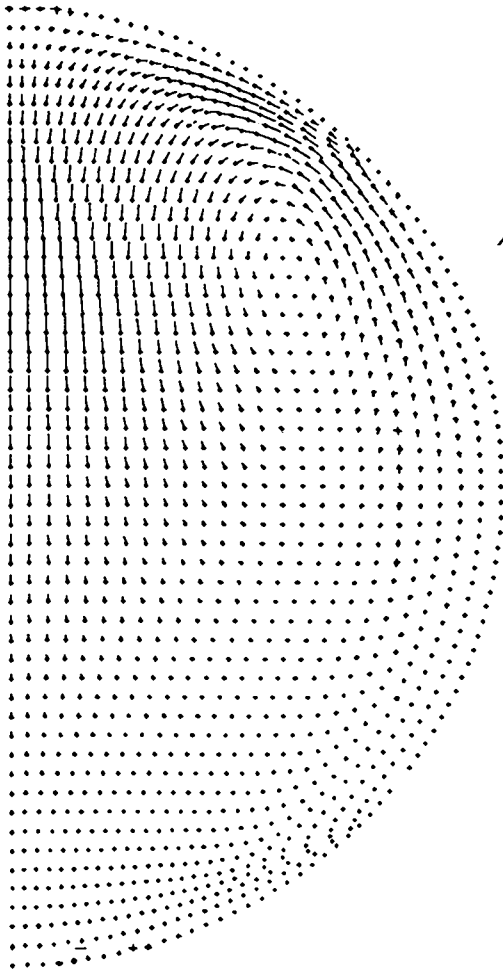


Fig. 7. Velocity vectors at 15 sec. The longest vector represents a speed of 23 m/sec. Each vector points away from "+" symbol at its base.

traverses the hot bubble. If the shock is expanding $v_{MAX} = v_S + v_R$, but during contraction $v_{MAX} = |v_S - v_R|$. In Fig. 6 we plot the minima (M), the expansion maxima (E), and the contraction maxima (C). Because the data occur at discrete intervals there is scatter. Appropriate envelopes have been drawn. The curves yield a rise rate of about 20 m/sec during the 4-to 8-sec time range. v_S , which is the material velocity in the shock as it traverses the hot bubble, drops from 100 m/sec at 2 sec to 40 m/sec at 8 sec. By 15 sec the shock is no longer recognizable and the circulation pattern is fully

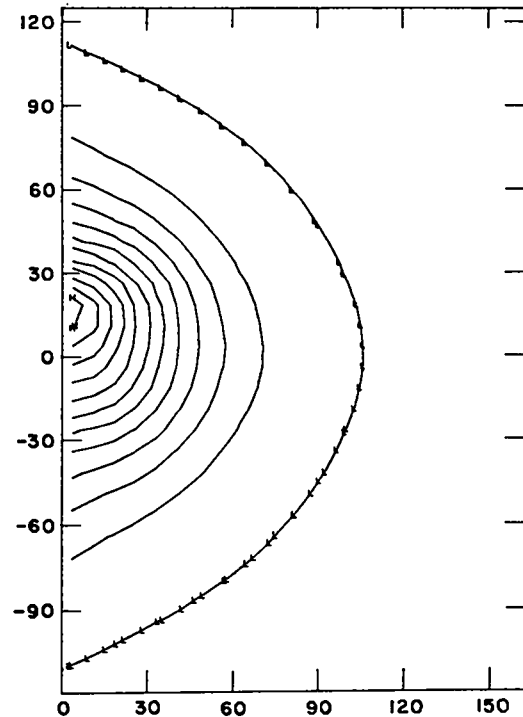


Fig. 8. Contours of specific internal energy at 1 sec. Successive contours have the ratio $10^{1/5} = 1.585$. The "L" contour is at 0.631×10^{10} erg/g. The coordinates are given in meters.

established. Figure 7 shows the 15 sec velocity vectors. The maximum velocity is 23 m/sec.

IV. TEMPERATURE AND LOCATION OF THE HOT BUBBLE

Figures 8, 9, 10, and 11 show specific internal energy contours at 1, 5, 10, and 15 sec, respectively. In particular, note that by 15 sec the hot bubble has reached the top of the cavity. The no-slip boundary condition effectively introduces an artificial boundary layer about 8 m thick. Detailed treatment of the cavity surface is required before the question of the temperature of the hottest material that comes into contact with the cavity surface can be answered. The present calculation should provide a lower limit. This is due, not only to the artificial boundary layer, but also to the apparently large amount of numerical diffusion that has significantly lowered the fireball temperature. Figure 12 shows the fireball temperature and

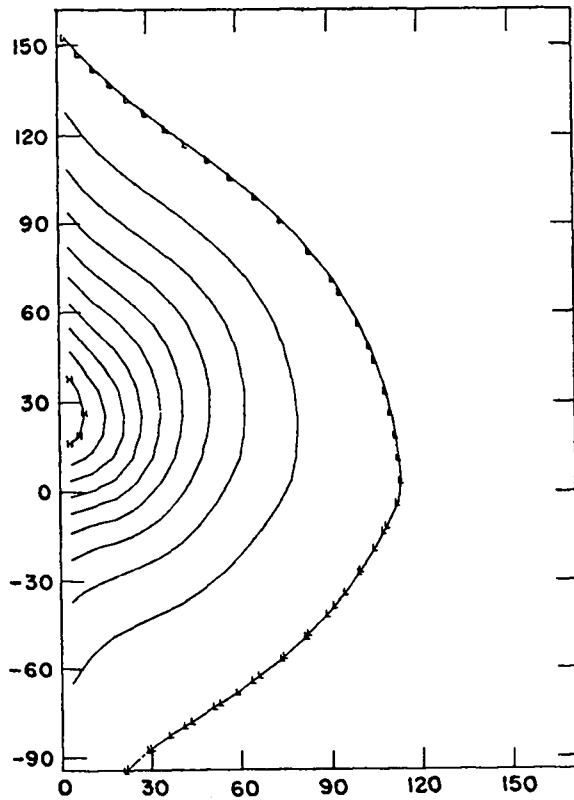


Fig. 9. Specific internal energy contours at 5 sec. "L" = 0.658×10^{10} erg/g, "H" = 4.33×10^{10} erg/g. The ratio of successive contours is $10^{1/11} = 1.233$.

location as a function of time. Figure 13 is a vertical profile of energy density at 0.15 and 10 sec. Considerable numerical diffusion has occurred. Nonetheless, we can say that at 12 sec material hotter than 1900°K is within 20 meters of the upper wall.

V. EVOLUTION AFTER 15 SECONDS

The present calculation was run with no-slip, reflective boundaries. The no-slip boundary condition is equivalent to assume a boundary layer of about one cell thickness (8 m). It is not at all certain what the turbulence state of the fluid will be. Therefore we quote the raw result that the circulation pattern takes on characteristics

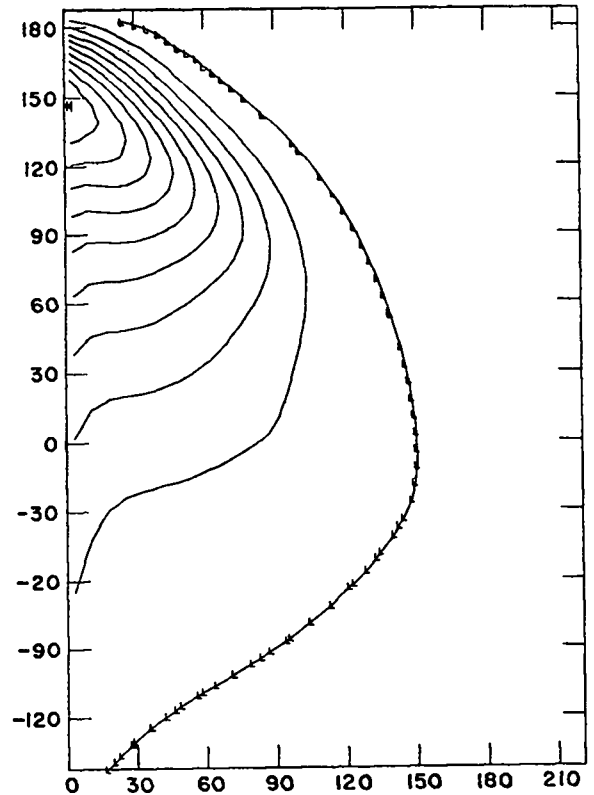


Fig. 10. Contours of specific internal energy at 10 sec. "L" = 0.60, "H" = 2.15 and $DQ = 1.136 = 10^{1/18}$.

of "sloshing" motion by 30 sec and persists for at least two minutes. Typical velocities are on the order of 5 -10 m/sec. The reader is again cautioned that the results after 15 sec are very dependent on boundary conditions.

VI. ACKNOWLEDGMENTS

The ease with which YAQUI was converted to the present use is due to those who developed the basic program: C. W. Hirt, A. A. Amsden, R. A. Gentry, H. M. Ruppel and other members of T-3. John Kodis and John Zinn are thanked for their RADFLO results.

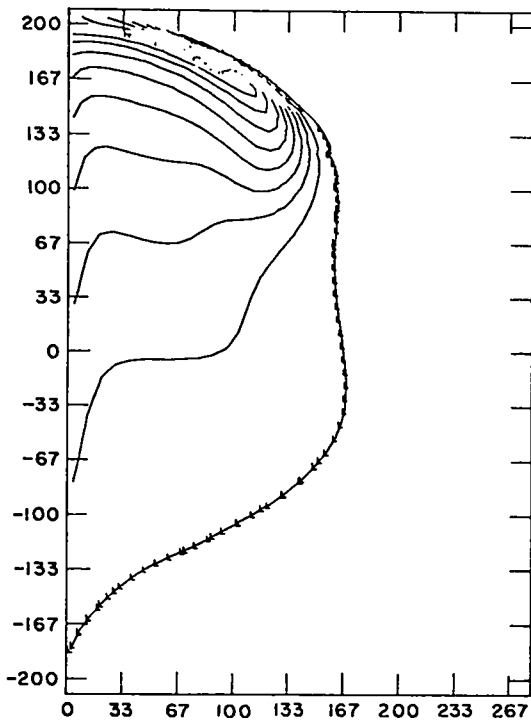


Fig. 11. Contours of specific internal energy at 15 sec. $L = 5.95 \times 10^{10}$ erg/g, $H = 1.16 \times 10^{10}$ erg/g and $DQ = 1.077 = 10^{1/31}$.

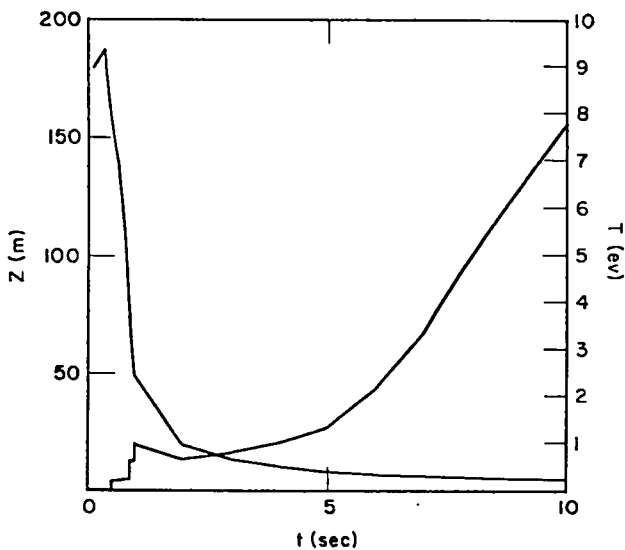


Fig. 12. Maximum temperature and the vertical displacement of that maximum as functions of time. At 10 sec this temperature is 0.22 eV.

CM:55(25)

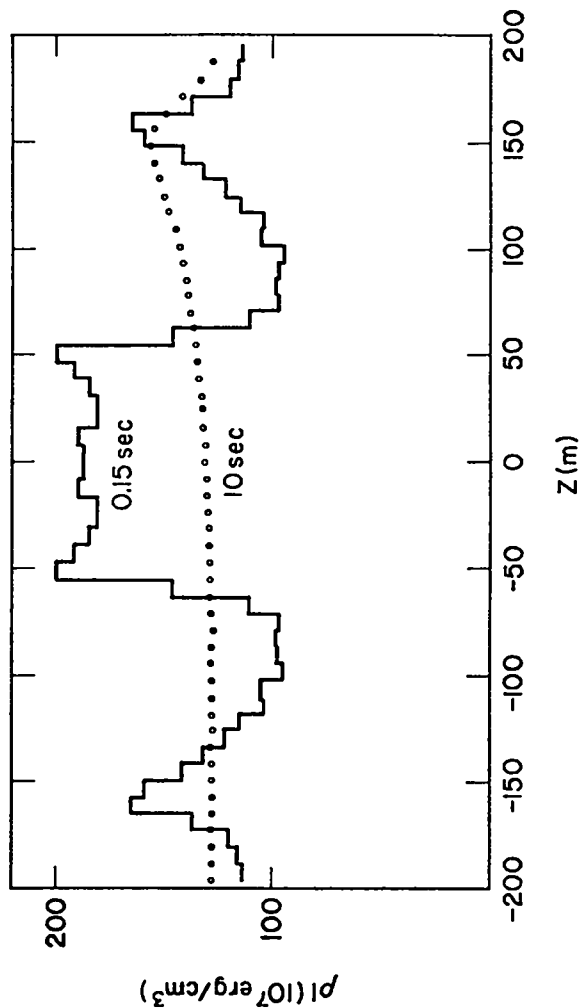


Fig. 13. Vertical profiles of energy density at 0.15 sec and 10 sec.

REFERENCES

1. C.W. Hirt and A.A. Amsden, "An Arbitrary Lagrangian-Eulerian Computing Method for All Flow Speeds," submitted to J. Comp. Phys. (1972).
2. A. A. Amsden and C. W. Hirt, "YAQUI: An Arbitrary Lagrangian-Eulerian Computer Program for Fluid Flow at All Speeds," LA-5100 (March 1973).
3. J. Zinn, "A Finite Difference Scheme for Time-Dependent Spherical Radiation Hydrodynamics Problems," submitted to J. Comp. Phys. (1972).
4. J. Zinn and J. W. Kodis, unpublished calculations.
5. J. Zinn, private communication.
6. A. A. Amsden and C. W. Hirt, "A Simple Scheme for Generating General Curvilinear Grids," J. Comp. Phys. 11, 348 (1973).
7. R. M. Davies and G. I. Taylor, "The Mechanics of Large Bubbles Rising Through Extended Liquids and Through Liquids in Tubes," Proc. Royal Soc., A200, 375 (1950).